Central configurations of identical masses lying along curves

Kevin A. O'Neil*

Department of Mathematical and Computer Sciences, The University of Tulsa, 800 Tucker Drive, Tulsa, Oklahoma 74104, USA

(Received 22 January 2009; published 9 June 2009)

A central configuration is an arrangement of point masses in which the net gravitational accelerations are proportional to the displacements from the center of mass. Here several families of central configurations are described consisting of a large number of identical masses that occupy one or more curves. The families are found numerically. These central configurations are regular, an algebraic condition that assures their persistence in the presence of small perturbing forces such as external fields or tethering forces. Both planar and nonplanar families exist; the planar central configurations are associated with (unstable) periodic solutions to the n-body problem. Similar configurations are exhibited for objects having pairwise interaction proportional to d^{-p} at distance d for p different from 2, such as point vortices.

DOI: 10.1103/PhysRevE.79.066601 PACS number(s): 45.20.−d, 45.50.Pk, 47.32.C−, 95.10.Ce

In the n-body problem of celestial mechanics, the term *central configuration* is used to denote an arrangement of masses in which the acceleration of each mass due to gravitational forces is proportional to the displacement from the center of mass. Central configurations play a distinguished role in the analysis of the n-body problem appearing as limiting configurations in certain motions and marking topological changes in configuration space of the level sets of an important conserved quantity [1–3]. Planar central configurations are the basis for the simplest periodic solutions of the n-body problem, the relative equilibria, in which each body moves in a uniform circular orbit around the center of mass. The three-body central configurations (associated with the names Euler and Lagrange) have been known for two centuries; they are significant in the structure of the solar system (Trojan asteroids) and have been exploited as parking orbits for space telescopes such as *SOHO* and *WMAP*.

Despite their importance, little is known about central configurations of more than a few masses. Planar central configurations containing up to $n=10$ identical masses have been investigated numerically [4,5], but the number of configurations grows rapidly with n; indeed, it has not been proved that the number is finite for $n>4$ [6–8]. For arbitrary n a planar central configuration can be formed by properly arranging the masses along a straight line [9] or at the vertices of a regular n-gon, as in the classical three-body configurations mentioned above. Configurations consisting of concentric rings of masses are also known to exist [10]. These configurations may be viewed as having all the bodies on one or more straight line segments or circles.

In this note several families of central configurations are described consisting of large numbers of identical masses lying on one or more curves. Both planar and nonplanar families exist; they are found numerically as solutions to a system of algebraic equations. The solutions form families in the sense that the distribution of mass varies in a continuous way as the number of masses is increased. The solutions are regular in that the derivative matrix of the defining system of equations (described below) is nonsingular; thus a careful application of interval arithmetic and the inverse function theorem should suffice to rigorously establish the existence of these configurations. The regularity also assures that the solutions will persist in the presence of perturbations to the system, such as a weak external gravitational field, tethering forces between adjacent masses, or replacement of one or more point masses by nonsymmetric mass density distributions. Indeed, configurations exist even when some of the parameters of the defining equations are varied over a wide range. The masses of the bodies, for example, need not be identical; interesting configurations are exhibited below in which one body is 20 times more massive than the others. Furthermore, it is shown that analogous central configurations exist when the inverse-square gravitational interaction is replaced by one with a different exponent such as the one giving the interaction between point vortices in an inviscid fluid. In the vortex case the limit $n\to\infty$ may be taken giving a relative equilibrium configuration of vortex sheets.

Let n bodies of mass M/n be found at positions $\mathbf{r}_i$, $1\le i \le n$. We fix the center of mass at the origin so that the positions satisfy $\Sigma \mathbf{r}_i=\mathbf{0}$. These point masses form a central configuration if for some nonzero constant λ the equations

$$\lambda^2\mathbf{r}_i = \frac{GM}{n}\sum_{j\neq i}\frac{\mathbf{r}_i-\mathbf{r}_j}{|\mathbf{r}_i-\mathbf{r}_j|^3}, \quad 1\le i\le n \tag{1}$$

are satisfied. Different values of λ merely reflect different scalings for the configuration, so it is sufficient to set $\lambda^2 = GM$ and use the system of equations

$$\mathbf{0} = \mathbf{f}_i := \mathbf{r}_i - \frac{1}{n}\sum_{j\neq i}\frac{\mathbf{r}_i-\mathbf{r}_j}{|\mathbf{r}_i-\mathbf{r}_j|^3}, \quad 1\le i\le n. \tag{2}$$

It is important to note that central configurations are determined by algebraic conditions, not dynamic ones.

For the moment, assume that all the bodies lie in a plane; we may write $\mathbf{r}_i=(x_i,y_i,0)$ for each i. Because the center of mass is fixed at the origin, there are only $n-1$ independent positions for the bodies. Also any solution to Eq. (2) will still be a solution after rotation of the configuration around the origin; let us assume a rotation that enforces the condition $y_1=0$. Thus there are $N=2n-3$ real variables $x_1,x_2,y_2,\ldots,x_{n-1},y_{n-1}$ available to satisfy system (2). On the

*FAX: (918) 631-3077; koneil@utulsa.edu

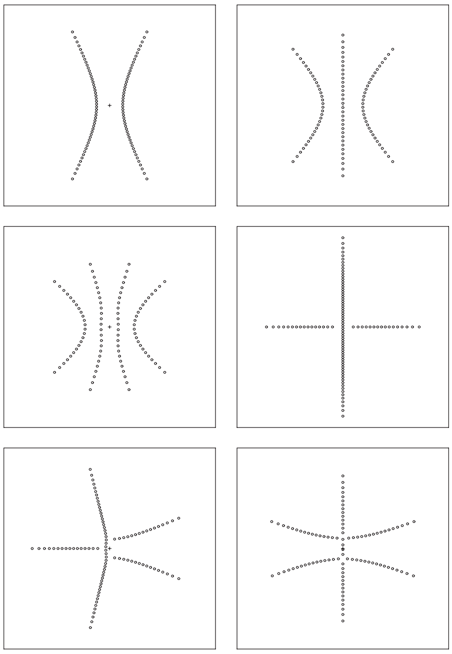

FIG. 1. Planar central configurations of 96 identical masses. The center of mass is marked by a cross.

other hand the sums $\Sigma \mathbf{f}_i$ and $\Sigma(\mathbf{r}_i \times \mathbf{f}_i)$ vanish independent of the positions $\mathbf{r}_1, \ldots, \mathbf{r}_n$ so that the system of equations (2) is equivalent to the vector equations $\mathbf{0}=\mathbf{f}_i$, $2 \leq i \leq (n-1)$, and the scalar equation $0=\mathbf{r}_1 \times \mathbf{f}_1$. Thus the system of n vector equations (2) reduces to the vanishing of N real functions in N real variables. The collection of all partial derivatives of the real functions with respect to these variables forms a $N \times N$ real derivative matrix that may be used to find central configurations.

Solutions to Eq. (2) were constructed numerically in the following way. The n masses were initially arrayed along selected curves with uniform spacing. A modified form of Newton's method that has global convergence properties [11] was then used to compute a sequence of new positions for which the $\mathbf{f}_i$ tend to zero. Specifically, the inverse of the derivative matrix is multiplied by a small parameter, slowing the rate of convergence of Newton's method but increasing the region of convergence. The process was continued until all the residuals $|\mathbf{f}_i|$ were reduced below a fixed threshold, typically 10^{-14}. Then the derivative matrix of the system was verified to be nonsingular indicating that the zero sets of the defining functions intersect transversely in N-dimensional space and hence that the positions computed are indeed approximations to an exact solution to the system. Because the bodies are closely spaced along the curves, the functions $\mathbf{f}_i$ are much more sensitive to displacements of the bodies in the directions tangent to the curves than perpendicular to them. The condition number of the derivative matrix was usually quite acceptable, however. For a typical solution with $n=100$, the largest singular value of this matrix is 600, the smallest is 0.5, and all but the smallest 15 are larger than 10.

Planar central configurations obtained in this manner are displayed in Figs. 1 and 3. Some are clearly related to the classical solutions mentioned above (all bodies on one line segment or one circle.) Figure 1 shows six relative equilibrium configurations of 96 identical masses that are found by the numerical scheme when the bodies are initially placed on several parallel or perpendicular line segments, generalizing Moulton's collinear configuration. These configurations appear to exist for all sufficiently large n generally requiring at minimum about ten masses on each line segment. For instance, the configuration in the upper left of Fig. 1 could not be found for n less than 16. There appears to be no upper limit for n in these families, although hardware and software limitations became evident for $n > 300$. A subtle dependence on n in the shape of the configurations appears when n is large, due to the fact that the net contribution to the acceleration of each body from the bodies in its immediate vicinity is proportional to $\kappa \ln(1/\delta)$, κ being the curvature of the curve on which they lie and δ the spacing between the bodies [12]. The result is that the masses tend to lie along slightly straighter arcs when n is very large. This effect is visible in Fig. 2, where central configurations are superimposed for the values $n=50$, 100, 200, and 300. In Fig. 3 a number of configurations are shown that are related to the classical n-gon (circular) configuration. The first is simply an oval with nonuniform mass distribution; the curve deviates from an ellipse by a few percent. Some masses may be placed along the major axis of the oval, as shown in the figure. When their

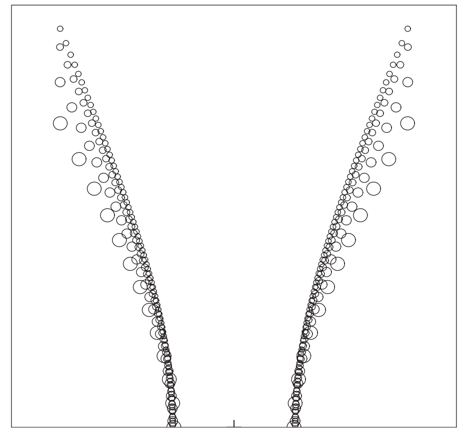

FIG. 2. Superposition of four central configurations with $n=50$, 100, 200, and 300. The area of each circle is proportional to $1/n$; only the upper half-plane is shown.

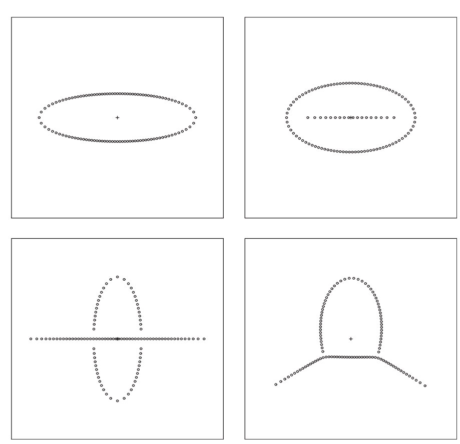

FIG. 3. Planar central configurations of 108 identical masses.

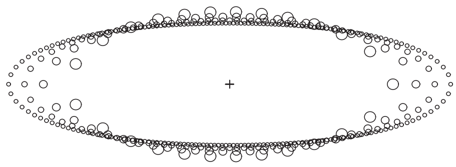

FIG. 4. Superposition of nearly elliptical planar central configurations with $n=25$, 50, 100, and 200. The area enclosed by each circle is proportional to the mass M/n.

number becomes great enough, the line segment pierces the oval. In this circumstance, the number of masses on either side of the segment may be changed; the segment will bend in response to any imbalance. The extreme case with no bodies at all on one side is displayed at lower right.

All of these configurations are regular solutions of system (2) in the sense that the derivative matrix of the reduced system is nonsingular. For this reason, Eq. (2) may be perturbed slightly and a corresponding perturbed solution configuration will exist. For instance, terms representing the tension τ in a tether joining adjacent bodies may be added to Eq. (2); for sufficiently small τ, a solution may be found by moving the bodies slightly from their zero-tension positions. Configurations such as these may prove useful for the design of tethered arrays of bodies (e.g., sensors) in a microgravity environment. One could also add a weak external gravitational field to obtain perturbed configurations; if the field is symmetric about the origin then planar configurations will also be associated with periodic solutions of the n-body problem.

The oval or nearly elliptical solutions deserve further discussion. The configuration is very close to an ellipse when n is large; for example, in the configuration with $n=120$ each mass position satisfies $(0.317x_i)^2+y_i^2=0.227+\delta_i$ with $|\delta_i| < 0.003$. Decreasing n leads to lower eccentricity as illustrated in Fig. 4. The oval central configuration with ten masses is quite difficult to distinguish from the circular configuration, as seen in Fig. 5. The mass positions are indicated by circles, while the dots show the vertices of a regular n-gon. (The oval configuration of ten masses was published earlier in a catalog of planar central configurations [4], but apparently not recognized as noncircular.) No oval configurations were found for n below 10.

Solutions to Eq. (2) in which the bodies do not all lie in a plane can also be found. The reduction from vector equations to real equations is similar to the planar case. A typical nonplanar central configuration is shown in plan and elevation views in Fig. 6. A great variety of such configurations can be found with ease.

It is interesting to consider solutions to the more general system of equations:

$$\mathbf{0} = \mathbf{r}_i - \sum_{j\neq i}\left(\frac{m_j}{M}\right)\frac{\mathbf{r}_i-\mathbf{r}_j}{|\mathbf{r}_i-\mathbf{r}_j|^{\alpha}}, \quad 1 \le i \le n. \tag{3}$$

Here the "mass" of the jth body is m_j and a parameter α has been introduced as the exponent of interaction; values of α different from 3 correspond to objects having different interaction potentials. Figure 7 displays some solutions to Eq. (3)

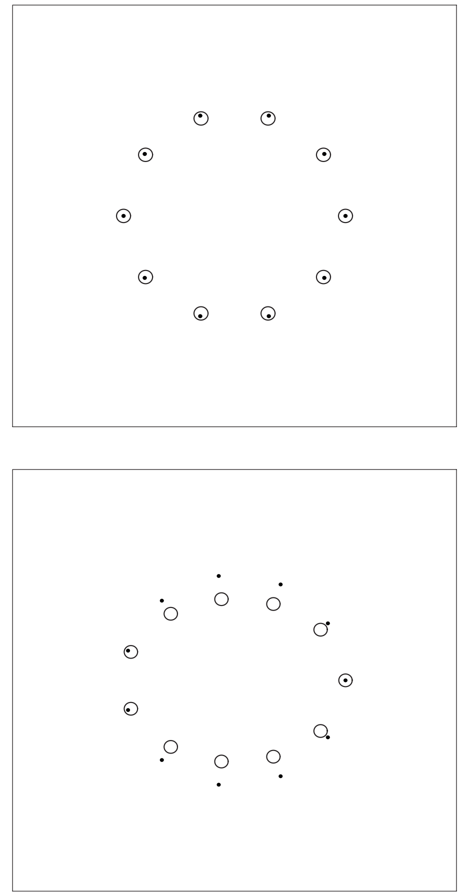

FIG. 5. A comparison of oval (circles) and circular (dots) central configurations with $n=10$ and $n=11$. For the $n=10$ oval configuration, the magnitude ratios $|\mathbf{r}_j|/|\mathbf{r}_1|$ take the values 1, 0.989 324, and 0.972 814.

with $n=60$. In the upper two configurations, the interaction is the same as in Eq. (2), $\alpha=3$, but one body is 20 times as massive as the others. (In the figure, the mass of each body is proportional to the area enclosed by its circle.) There are many different configurations possible. As the one large body is made more and more massive, the smaller bodies eventually lie on radial line segments only. The equations may be further perturbed by using a nonsymmetric mass density distribution rather than a point mass to calculate the gravitational force due to the largest body; this could take into account the oblateness of a heavenly body, for example. Experimentation shows that the perturbation can be substantial without gross deformation of the overall central configuration. The lower two configurations show variations in configuration shape with identical m_i but changes in α. The lower left configuration was computed with $\alpha=2$, corresponding to the interaction between point vortices in a two-dimensional fluid, the m_i now being the vortex intensities. Many relative equilibria of point vortices have been computed [13] including families with the vortices lying on concentric circles [14]. In contrast to the gravitating case, the sum in Eq. (3) has no divergent local contribution when $\alpha < 3$; in the limit $n\to\infty$ the sum becomes a convergent principal-value integral over a one-dimensional distribution

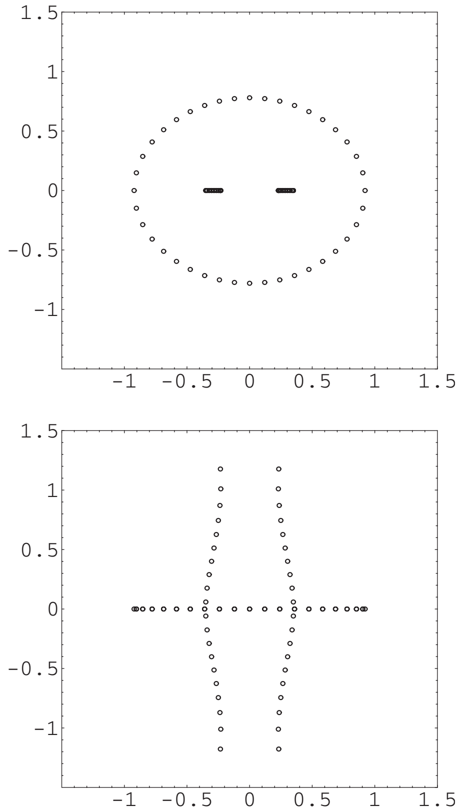

FIG. 6. A nonplanar central configuration with $n=80$. The upper figure is the plan view, i.e., a projection onto the xy plane with the x axis running vertically. The lower figure is the elevation view, the projection onto the yz plane.

of vorticity, i.e., one or more vortex sheets. Computations of solutions to Eq. (3) with increasing n show numerical convergence to sheets [15], and vortex sheet relative equilibria have been observed in a rotating superfluid [16,17]. The configuration shown in the lower right was computed with $\alpha=4$, so that the interaction force drops off more rapidly with distance than gravitation. Most of the relative equilibria shown in Figs. 1 and 3 have analogs for α as large as 10.

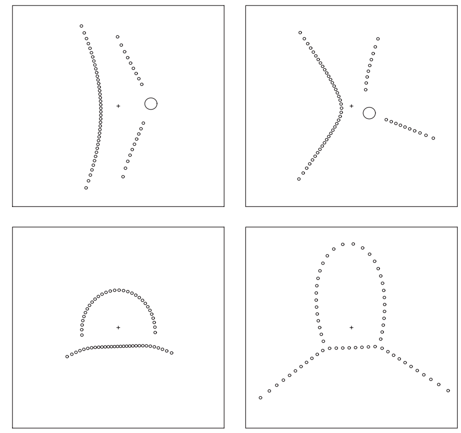

FIG. 7. Solutions to Eq. (3) with $n=60$. Upper: large body is 20 times as massive as the others. Lower: $\alpha=2$ (left) and $\alpha=4$ (right).

In summary, families of central configurations have been shown to exist in which large numbers of identical masses are arranged along curves; both planar and nonplanar configurations can be found. These configurations have an algebraic regularity property that assures existence in the presence of small perturbations to the system such as tethering forces. Beyond this property, direct computation has shown that the perturbations may be large: the masses may vary over a wide range and even the interparticle interaction itself may be changed considerably. The corresponding configurations of point vortices have been considered elsewhere [15].

Any planar central configuration gives rise to a family of homographic motions [1], with the zero angular momentum collision motion at one extreme and the periodic motion (relative equilibrium) at the other. For the configurations considered in this paper the relative equilibria are unstable in general, just as is the case with the Lagrange and Euler three-body motions. There is an additional source of instability for configurations with masses closely spaced along a curve: simulations indicate that even extremely small velocity perturbations can cause adjacent masses to collide, so that the motion becomes singular in a short time. In some ways the situation is comparable to the roll-up of a vortex sheet [15].

[1] A. Wintner, *The Analytical Foundations of Celestial Mechanics* (Princeton University Press, Princeton, NJ, 1941).
[2] S. Smale, Invent. Math. **11**, 45 (1970).
[3] D. G. Saari, Celestial Mech. **40**, 197 (1987).
[4] D. Ferrario, e-print arXiv:math/0204198.
[5] A. Chenciner, *Proceedings of the ICM, Beijing, 2002*(Higher Education Press Beijing, China, 2002), Vol. 3, pp. 255–264.
[6] S. Smale, Math. Intell. **20**, 7 (1998).
[7] M. Hampton and R. Moeckel, Invent. Math. **163**, 289 (2006).
[8] G. Roberts, Physica D **127**, 141 (1999).
[9] F. R. Moulton, Ann. Math. **12**, 1 (1910).
[10] D. G. Saari, *Collisions, Rings and Other Newtonian N-Body Problems* (American Mathematical Society, Providence, RI, 2005).
[11] M. Hirsch and S. Smale, Commun. Pure Appl. Math. **32**, 281 (1979).
[12] G. Buck, Nature (London) **395**, 51 (1998).
[13] H. Aref, P. Newton, M. Stremler, T. Tokieda, and D. Vainchtein, Adv. Appl. Mech. **39**, 1 (2003).
[14] H. Aref and M. van Buren, Phys. Fluids **17**, 057104 (2005).
[15] K. O'Neil, Physica D **238**, 379 (2009).
[16] E. V. Thuneberg, Physica B **210**, 287 (1995).
[17] M. T. Heinila and G. E. Volovik, Physica B **210**, 300 (1995).